Food and Chemical Toxicology 143 (2020) 111514

Contents lists available at ScienceDirect

Food and Chemical Toxicology

journal homepage: www.elsevier.com/locate/foodchemtox

Phosmet bioactivation by isoform-specific cytochrome P450s in human hepatic and gut samples and metabolic interaction with chlorpyrifos

Nicoletta Santori[a], Franca Maria Buratti[a,*], Jean-Lou C.M. Dorne[b], Emanuela Testai[a]

[a] Istituto Superiore di Sanità, Environment & Health Dept., Viale Regina Elena, 299, 00161, Roma, Italy
[b] EFSA (European Food Safety Authority), Scientific Committee and Emerging Risks Unit, Via Carlo Magno, 1A., 43126, Parma, Italy

ARTICLE INFO

Keywords:
Phosmet
Human biotransformation
Toxicokinetics
Cytochromes P450 isoforms
Inhibitors
Chemical interaction

ABSTRACT

Data on the bioactivation of Phosmet (Pho), a phthalimide-derived organophosphate pesticide (OPT), to the neurotoxic metabolite Phosmet-oxon (PhOx) in human are not available. The characterization of the reaction in single human recombinant CYPs evidenced that the ranking of the intrinsic clearances was: 2C18 > 2C19 > 2B6 > 2C9 > 1A1 > 1A2 > 2D6 > 3A4 > 2A6. Considering the average human hepatic content, CYP2C19 contributed for the great majority (60%) at relevant exposure concentrations, while CYP2C9 (33%) and CYP3A4 (31%) were relevant at high substrate concentration. The dose-dependent role of the active isoforms was confirmed in human liver microsomes by using selective CYP inhibitors. This prominent role of CYP2C in oxon formation was not shared by other OPTs. The pre-systemic Pho bioactivation measured in human intestinal microsomes was relevant accounting for ¼ of that measured in the liver showing two reaction phases catalysed by CYP2C and CYP3A4. Phosmet efficiently inhibited CPF bioactivation and detoxication, with Ki values (≈30 μM) relevant to pesticide concentrations achievable in the human liver, while the opposite is unlikely (Ki ≈ 160 μM) at the actual exposure levels, depending on the peculiar isoform-specific Pho bioactivation. Kinetic information in humans can support the development of quantitative *in vitro/in vivo* extrapolation and in silico models for risk assessment refinement for single and multiple pesticides.

1. Introduction

The potential correlation between exposure to organophosphate insecticides (OPTs) and neurodegerative diseases (e.g. Parkinson's disease) and/or neurodevelopmental effects have been extensively discussed in the last years (Sánchez-Santed et al., 2016). Based on human health concern associated with their neurotoxic effects, many OPTs have been withdrawn from the EU market (e.g. dimethoate, parathion and malathion). Therefore, increasing attention has been raised for those OPTs still commercialised, such as Phosmet (Pho), a phthalimide-derived OPT (Fig. 1) applied on fruit trees, ornamental plants, other crops and on animals for pest control.

Kinetic and metabolism data are available in the scientific literature on a number of OPTs and, despite showing different chemical structures, similar metabolic pathways have been observed (Butler and Murray, 1997; Mutch et al., 1999; Kappers et al., 2001; Tang et al., 2001; Buratti et al., 2002, 2003, 2005). One common reaction is OPT bioactivation to the toxic metabolite, generally named oxon, requiring an oxidative desulfuration reaction mediated by cytochrome P450 (CYP450). The oxon acts via acetylcholinesterase (AChE) inhibition, the specific key event leading to the neurotoxic effects of this class of insecticides. Some OPTs can also be i) biotransformed by Flavin-containing Mono-Oxygenases (FMO), when a second sulfur atom is present; ii) detoxified by CYP450 isoforms (CYPs) and/or esterases to non-toxic metabolites (Buratti and Testai, 2007; Leoni et al., 2008). After biotransformation, alkyphosphates such as dimethyldithiophosphate, dimethylthiophosphate and dimethylphosphate are extensively excreted in the urine and have been used as biological markers of exposure to OPTs (Aprea et al., 1998, 2004).

Concerning Pho, very limited specific information is reported in the open literature. Basic reactions have been proposed for its metabolism in rats including: oxidation to phosmet-oxon (PhOx) mediated by CYP450 isoforms, thiophosphoryl hydrolysis, S-methylation, oxidation to form sulfoxide and sulfone likely mediated by FMO (Fig. 1) (EFSA, 2011), but no information is available for human metabolism.

Considering the increasing importance given to *in vitro* comparative metabolism between human and test species (rat, mouse, dog, rabbit), which, following Commission Regulation EU No 283/2013, has become a data requirement for active substances to be used in plant protection products, this work aims to characterise *in vitro* the human CYP450

* Corresponding author
E-mail address: franca.buratti@iss.it (F.M. Buratti).

https://doi.org/10.1016/j.fct.2020.111514
Received 28 March 2020; Received in revised form 6 May 2020; Accepted 3 June 2020
Available online 23 June 2020

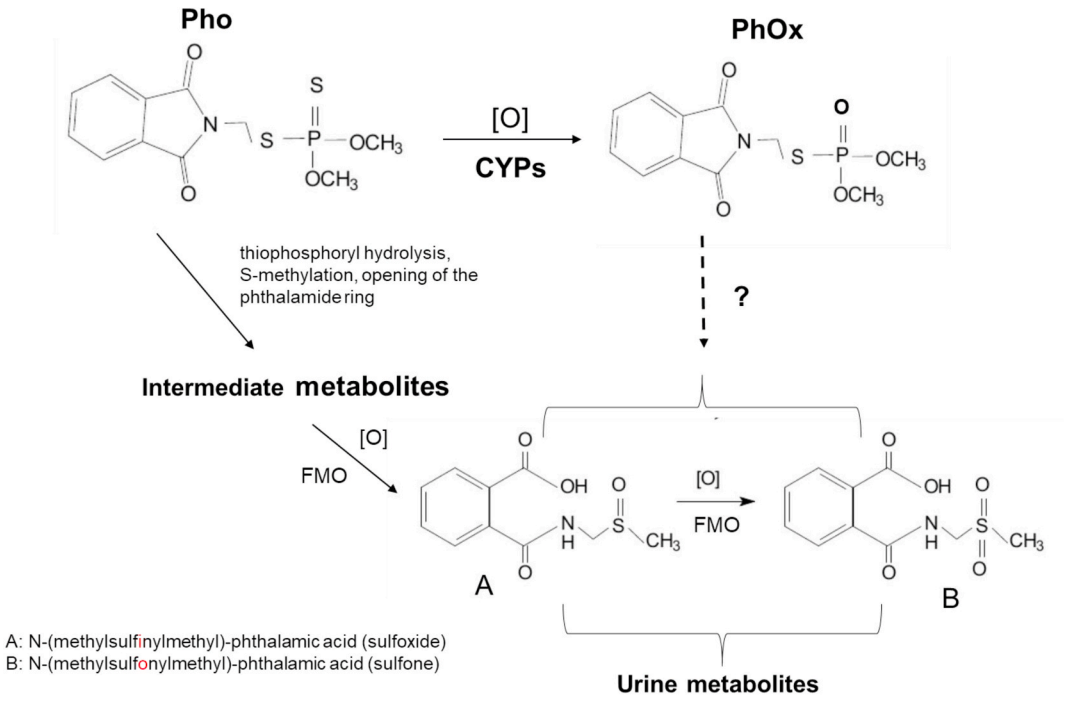

Fig. 1. Pho and PhOx chemical structures and proposed metabolic pathway.

isoforms involved in Pho bioactivation to PhOx. Here, kinetic parameters including maximum velocity (Vmax), Michealis-Menten constant (Km) to derive the intrinsic clearances (CLi) of PhOx formation were determined in single human recombinant isoforms (CYP2C18, 2C19, CYP 2B6, CYP 2C9, CYP1A1, CYP1A2, CYP2D6, CYP3A4, CYP2A6, CYP 2C8), human liver microsomes (HLM), human intestinal microsomes (HIM). Specific chemical inhibitors were also tested to confirm the involvement of specific CYP isoforms in PhOx formation. Finally, since the general human population may be co-exposed to different OPTs, possible metabolic interactions between Pho and Chlorpyrifos (CPF) through CYP inhibition was also investigated.

The study is part of an EFSA funded project (GP/EFSA/SCER/2015/01) which aims to identify and model human variability in toxicokinetics (TK) and metabolism, while filling the data gaps on isoform-specific metabolism for compounds of relevance to food safety to better inform human physiologically-based kinetic (PB-K) models and support their use in chemical risk assessment.

2. Material and methods

2.1. Chemicals

Phosmet (Pho) was supplied by Sigma-Aldrich (Saint Louis, MO), purity ≥ 98%. phosmet-oxon (PhOx) (purity 95%). Chlorpyrifos (CPF) (purity 98,8%), Chlorpyrifos-oxon (CPFO) (purity 95%) and 3,5,6-trichloro-2-piridinol (TCP) (purity > 98%). were purchased by Chem-Service (WestChester, PA). Roche GmBh (Mannheim, Germany) supplied NADP, glucose-6-phosphate (G6P) and G6P-dehydrogenase (G6PDH), while $MgCl_2$ hexahydrate was purchased from J.T. Baker (Deventer, NL). All other analytical grade products were obtained by commercially available sources. The isoform-selective CYP450 inhibitors Ticlopidine (TIC), Sulfaphenazole (SUL) and Ketoconazole (KETO) were supplied by Sigma-Aldrich (St. Louis, MO).

2.2. Biological samples: recombinant human CYPs, human liver microsomes (HLM) and human intestinal microsomes (HIM)

cDNA-recombinant human CYPs, prepared from *Escherichia coli*-infected cells expressing single isoforms (1A1, 1A2, 2A6, 2B6, 2C8, 2C9, 2C19, 2D6, 2C18 and 3A4), were purchased from Xenotech (Lenexa, KS). The protein content was of 10 mg/mL and CYP450 content was 1 nmol/mL, as indicated by the supplier. HLM from hepatic biopsies pooled from 200 donors (100 male and 100 female) and HIM from 15 mix gender donors were obtained by Xenotech (Lenexa, KS). Protein concentration in HLM and HIM was 20 mg/mL (355 pmol CYP450/mg protein) and 10 mg/mL, respectively. HLM and HIM were fully characterized by the supplier for the main monooxygenase activities by using selective model substrates for single CYPs (Table 1).

2.3. In vitro metabolism of Pho to PhOx by recombinant human P450, HLM and HIM

2.3.1. Enzymatic incubation for PhOx formation

The standard incubation mixture was prepared in borosilicate test tubes (final volume 250 μL) using 0.16M G6P, 0.12M $MgCl_2$, 2–4 U/mL G6DPH, 1 mM NADP, and 50–100 pmol CYP450/mL for the recombinant enzyme or 1 mg microsomal protein/mL when HLM and HIM were tested, in 50 mM Tris-HCl and 1 mM EDTA (pH = 7.4). Pho was tested at 6–9 different concentrations (range 0.5–300 μM), at 37 °C, under shaking (80 cycle/minute). The stability of Pho in the stock and working solution was tested: as a result, the stock solution was prepared every two weeks, whereas the working solution was freshly prepared

Table 1
CYPs marker activity in HLM.

	1A2	2A6	2B6	2C8	2C9	2C19	2D6	3A4/5
HLM	530	1650	673	2080	2100	89.3	229	2940
HIM								951

Results are expressed as pmol · (mg prot· min)$^{-1}$
Marker activity used by the supplier for HLM characterization: Phenacetin O-dealkylation (CYP1A2), Coumarin 7-hydroxylation (CYP2A6), Bupropion hydroxylation (CYP2B6), Amodiaquine N-dealkylation (CYP2C8), Diclofenac 4′-hydroxylation (CYP2C9), S-Mephenytoin 4′-hydroxylation (CYP2C19), Dextromethorphan O-demethylation (CYP2D6), Testosterone 6β-hydroxylation (CYP3A4/5).

every week.

Preliminary studies were carried out testing various incubation times (15, 30, 60 and 120 min) and protein content (0.5, 1 and 2 mg/mL) to define experimental condition within the linearity of the enzymatic reaction (data not shown). The selected incubation times were: 15 min for CYP2C19, 2C18 and HLM; 30 min for CYP2B6 and HIM; 60 min for any other CYPs. The mixture was pre-incubated at 37 °C for 3 min before starting the reaction by adding the substrate; at the end of the incubation time, it was blocked by adding ice-cold MeOH (125 μL). Before HPLC analysis, samples were centrifuged at 8000 rpm 4 °C for 10 min, using a refrigerate 5417R Eppendorf Centrifuge, to separate proteins from the supernatant. If not analyzed immediately, samples were stored at −20 °C, for a maximum of 24 h. The recovery for Pho and PhOx was > 85% (data not shown). At least three independent experiments were carried out using different vials as the enzyme source.

The non-enzymatic Pho degradation in the incubation conditions was estimated running blanks in the absence of NADP: after 1 h the reduction was ≤15% of the starting dose, being not relevant in our experimental conditions.

2.3.2. Enzymatic incubation with CYP inhibitors

In order to study the contribution of different CYPs in HLM, the effect of ticlopidine (TIC, 20 μM) a specific inhibitor for CYP2C19 and CYP2B6, sulphafenazole (SUL, 10 μM), 2C family (mainly 2C9) specific inhibitor and Ketoconazole (KETO, 10 μM) a specific inhibitor for CYP3A4, were added to the incubation standard mixture. In order to verify their relative role, they were tested as: TIC alone, TIC + SUL and TIC + SUL + KETO. Inhibitor concentrations were chosen to theoretically suppress > 80% of the specific CYP activity, based on published Ki values. SUL was diluted in Tris-HCl buffer; TIC and KETO were dissolved in methanol (final MeOH concentration in the incubation < 0.5%). Since TIC is known to be a mechanism based inhibitor, it was added to the standard mixture and pre-incubated with HLM for 15 min at 37 °C before starting the reaction adding Pho (15 and 200 μM), then incubation was carried out at 37 °C for 15 min. SUL and KETO, which are known to act as competitive inhibitors, were added just before adding Pho. Blanks and control samples (without inhibitors) were carried out in parallel. At the end of the incubation time, the reaction was blocked by adding ice-cold MeOH (125 μL). Samples were centrifuged and analyzed using the HPLC method described below. At least three independent experiments were carried out using different vials, of the same pool, as the enzyme source.

2.4. Metabolic interaction Pho-CPF

In order to investigate the potential metabolic interaction between Pho and CPF through isoform-specific CYP inhibition, incubation with HLM were carried out as follows: i) Pho was used as a mechanism-based inhibitor of CPFO and TCP formation. After 15 min pre-incubation at 37 °C with Pho (0–60 μM), CPF (15–300 μM) acting as the substrate was added to the standard incubation mixture, which was then incubated for additional 5 min. ii) CPF was used as a mechanism-based inhibitor of PhOx formation. After 5 min incubation of the standard mixture with CPF (0–300 μM) at 37 °C, Pho (30 and 100 μM) was added and the incubation was run for additional 15 min. iii) CPF was used as a competitive inhibitor: the two pesticides were concomitantly added to the standard incubation mixture, which was then incubated for 15 min. Incubation time for CPF was chosen on the basis of previous studies (Buratti et al., 2003). In both cases, the reaction was blocked with ice-cold MeOH (125 μL); samples were centrifuged and analyzed using the HPLC method described below. At least three independent experiments were carried out using different vials, of the same pool, as the enzyme source.

2.5. HPLC analysis of PhOx, TCP and CPFO

HPLC analysis was applied to identify and quantify PhOx, TCP and CPFO formation, using a PerkinElmer Series 200 Liquid Chromatograph, equipped with a PerkinElmer diode array LC 235 detector and a Restek Pinnacle C-18 DB reversed-phase column (length = 25 cm, diameter = 4.6 mm).

Conditions for Pho and PhOx analysis were set up and were as follows: 1 mL/min flow rate, 20 μL injection volume and a mobile phase consisting of a MeOH/H_2O mixture 50:50 (v/v) for 5.5 min; 5 min of linear gradient to obtain a 70:30 ratio (v/v) of the MeOH/H_2O mixture; then after 3 min, a linear gradient was applied for 5 min, to return to the initial conditions. Retention times (Rt) were: 5.8 min (PhOx) and 13 min (Pho) and λ = 224 nm was used for detection. The amount of PhO and PhOx was determined referring to a calibration straight line (correlation coefficient R^2 = 0.996 for PhOx; R^2 = 0.988 for Pho), prepared with at least 7 known amounts of the analytical standards (0.5–50 μM). The coefficient of variation was 1% for Pho and 3.2% for PhOx. The limit of detection was < 0.1 μM for both PhO and PhOx and the limit of quantification was 0.27 and 0.24 μM for Pho and PhOx, respectively.

The concentration of CPF and its metabolites was tested by adapting a previously described method (Buratti et al., 2006). Conditions for CPF, CPFO e TCP analysis were as follows: injection volume 20 μL; flow rate 1 mL/min; the mobile phase consisted of MeOH:incubation buffer mixture (70:30, v/v) for 4.5 min, 80:20 (v/v) for 13 min, then the initial condition was restored and maintained for 3 min. Retention times were: 3.65 min (TCP), 9 min (CPFO) and 17.3 min (CPF). The absorption of the eluate was measured continuously at 325 nm for TCP and at 290 nm for CPFO and CPF. The amount of CPF and its metabolites was determined referring to a calibration straight line (correlation coefficient R^2 = 0.944, R^2 = 0.999 and R^2 = 0.992 for CPF, CPFO and TCP, respectively), prepared with at least 7 known amounts of the analytical standards (1–100 μM). The coefficient of variation was 7.1% for CPF, 6.8% for CPFO and 4.2% for TCP.

2.6. Data analysis

Kinetic parameters (Km and Vmax) were generated from linear and non-linear (Michaelis–Menten) regression fit with GraphPad 6 Prism™ software (GraphPad Software Inc., San Diego, CA). The intrinsic clearance (CLi) was obtained as the slope of the linear regression of the enzymatic activity curve, or as the Vmax/Km ratio for non-linear activities. The same software was used to determine the inhibition constant (Ki) when either CPF or Pho were used as reciprocal inhibitors, through investigating the most appropriate fit of the enzyme activity curves (non-competitive, competitive or uncompetitive). The IC_{50} value was calculated using linear regression by plotting % inhibition vs inhibitor concentrations. Paired t tests were performed to characterise the statistical significance of the inhibition ($p < 0.05$).

3. Results

3.1. Metabolism of Pho by single recombinant CYP450 isoforms

In the range of used substrate concentrations (0.5–300 μM Pho) all studied recombinant CYPs were active, except for CYP2C8, showing a very low activity, with only trace of PhOx detected (data not shown). Active CYPs had different kinetics: CYP1A2, CYP1A1, CYP2B6, CYP2C9, CYP2C18 and CYP2C19 showed a typical saturation curve (Fig. 2A and B), whereas CYP2A6 remained linear at the highest concentration tested (data not shown); other CYPs such as CYP3A4 and CYP2D6, showed an allosteric sigmoidal curve fitting (Fig. 2C and D), with a Hill coefficient of about 1.4 each (Table 2).

For all active CYPs, the kinetic parameters were calculated and reported in Table 2.

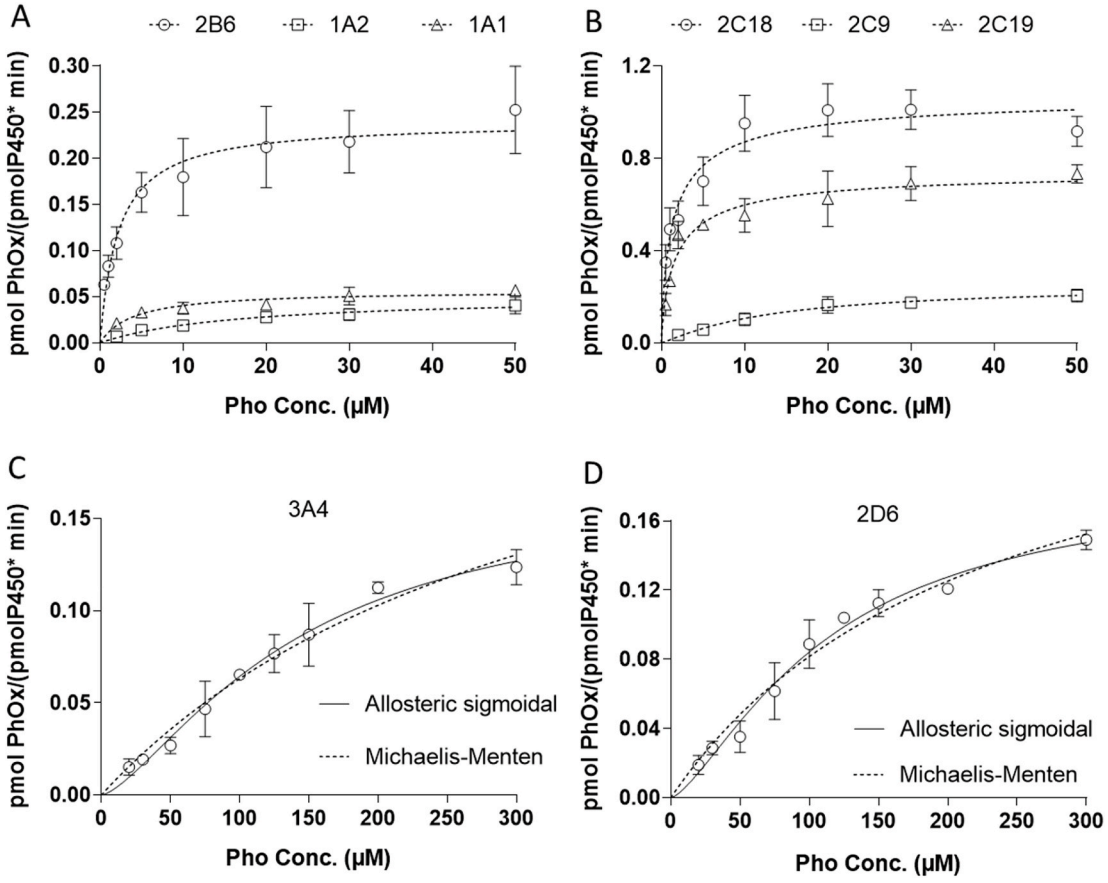

Fig. 2. Dependence of Pho metabolism catalysed by single recombinant CYPs on substrate concentration. Panels C and D reports those CYPs characterized by a allosteric sigmoidal curve. Results are expressed as pmol PhOx (pmolP450· min)$^{-1}$ and represent the mean ± SD on at least 3 independent determinations. Details of the experimental conditions were described under Materials and Methods.

Table 2
Kinetic parameters of PhOx formation by single active human recombinant CYPs, human liver microsomes (HLM) and human intestine microsomes (HIM).

CYPs[a]	Michaelis –Menten curve fitting			Allosteric sigmoidal curve fitting			
	Vmax	Km	Cli	h[c]	Vmax	Khalf[d]	Cli
2C18	1008	1.288	782.6				
2C19	702.3	1.496	469.4				
2B6	239.6	2.195	109.1				
2C9	273.8	16.01	17.1				
1A1	56.8	4.01	14.2				
1A2	51.4	16.44	3.1				
2D6	*269.1*	*229.7*	*1.2*	1.425	184.1	112.8	1.6
3A4	*278.4*	*340.7*	*0.8*	1.441	169.5	140.4	1.2
2A6			0.4				
HLM[b]	86	20.22	4.2				
HIM[e]	18.25	19.09	0.96				
	32.4	*103.9*	*0.3*				

[a] Vmax is expressed as pmol product/(nmolP450 · min); Km or Khalf is expressed as μM; Cli is expressed as pmol product/(nmolP450 · min · μM), it is the ratio Vmax/Km or Vmax/Khalf.

[b] Vmax is expressed as pmol product/(mg prot · min); Km is expressed as μM; Cli is expressed as pmol product/(mg prot · min · μM).

[c] Hill coefficient, when n = 1 it means Non-cooperative (completely independent) binding, which can be modeled by a classic Michaelis-Menten kinetics, when n > 1 Positively cooperative (allosteric) binding.

[d] Khalf is the concentration of substrate that produces a half-maximal enzyme velocity, as Km in the Michaelis -Menten.

[e] Kinetic parameters fo high and low affinity phase (the latter in italics). Vmax is expressed as pmol product/(mg prot · min); Km is expressed as μM; Cli is expressed as pmol product/(mg prot · min · μM).

The CLi values varied between 0.4 and 782.6 pmol PhOx/(nmolP450· min· μM) with the following ranking CYP2C18 > CYP2C19 > CYP2B6 > CYP2C9 > CYP1A1 > CYP1A2 > CYP2D6 > CYP3A4 > CYP 2A6.

To roughly estimate the relative CYP contribution (%) to total PhOx formation, a tentative extrapolation has been carried out, taking into account the average human hepatic content of each isoform, considering data reported in Pastrakuljic et al. (1997) and in Achour et al. (2014). The relative contribution of each CYP isoform was calculated starting from CL*i* values or *V*max for low and high Pho concentrations, respectively. For CYP1A6, the rate at 300 μM was used because Vmax could not be determined, being linear in the range of tested concentrations. When allosteric sigmoidal curves were demonstrated, the corresponding kinetic parameters were used for calculations. Results show that at low Pho concentrations, CYP2C19 was the isoform mainly involved in PhOx formation (60%), followed by CYP2B6 (20%). Conversely, at high substrate concentration CYP2C9 and CYP3A4 accounted for 33 and 31%, respectively, while the relative contributions of CYP2C19 and CYP2B6 were significantly lower (15% and 8%, respectively) (Fig. 3A and B). The relative contribution to PhOx formation of the other isoforms was below 5%. It is worth of note that, despite CYP2C18 was characterized by the highest Cli, its relative contribution was minor due to its very low hepatic content (0.1%) (Fig. 3A and B).

3.2. Pho metabolism by HLM and HIM

Using HLM from 200 donors, a typical saturation curve fitting with a Michaelis-Menten kinetic was obtained in the range of concentrations tested (0.5–300 μM) (Fig. 4A). The CLiapp was 4.2 pmol product/(mg

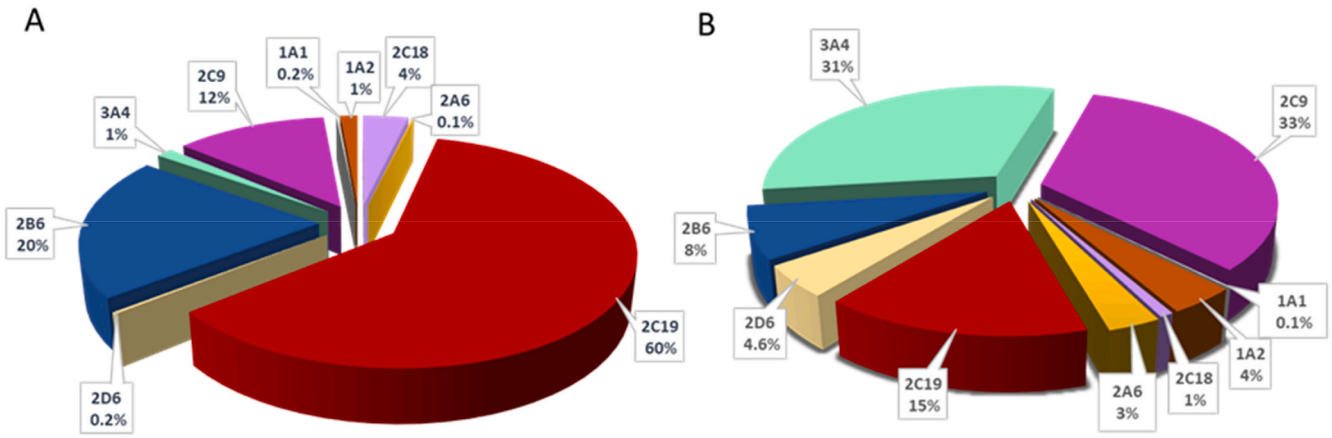

Fig. 3. Estimate of the relative contribution of CYP isoforms to PhOx biotransformation, using kinetic parameters obtained with recombinant enzymes and CYPs hepatic content (data from Pastrakuljic et al., 1997 and Achour et al., 2014) at low (A) and high (B) Pho concentrations.

prot·min·μM) (Table 2), two order of magnitude lower than the Cli for the most active recombinant isoform (CYP2C19).

When HIM were tested, an atypical kinetic curve was observed (Fig. 4B), which on the basis of the double straight lines obtained in the Eadie-Hofstee plot (Fig. 4B) could be interpreted as the result of two phases. Therefore, two CLiapp, 0.96 and 0.3 pmol product/(mg prot · min · μM) were derived for the high and low affinity phase, respectively (Table 2).

Results obtained by using specific chemical inhibitors indicated that at low Pho concentrations, the inhibition due to TIC alone reached 60%; when TIC and SUL were present inhibition increased up to 80%, while the further addition of KETO was ineffective (Fig. 5A). At high Pho concentration, each inhibitor gave a contribution to the inhibition of around 20–30%, reaching a total bioactivation reduction by 70% (Fig. 5B).

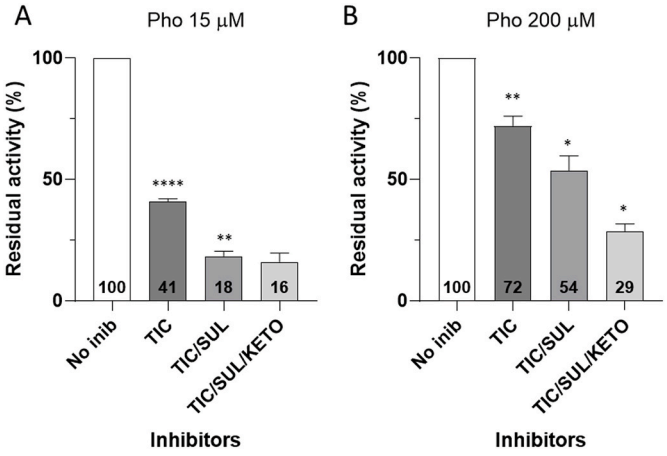

Fig. 5. Inhibition of Pho metabolism by isoform-specific CYP inhibitors with HLM at two different Pho concentrations: 15 μM (A) and 200 μM (B). Stars indicate the statistically significant difference when comparing: i) control incubation (without the inhibitor, set as 100% activity) vs incubation with TIC, ii) incubation with TIC vs incubation with TIC + SUL, iii) incubation with TIC + SUL vs TIC + SUL + KETO. * = $p < 0.05$; ** = $p < 0.01$; *** = $p < 0.005$; **** = $p < 0.0001$.

3.3. Metabolic interaction between Pho and CPF in HLM

OPT desulfuration results in the production of activated sulfur atoms, which then bind irreversibly those specific CYPs catalyzing the reaction, acting as mechanism based inhibitor (Butler and Murray, 1997; Halpert et al., 1980; Norman et al., 1974). Hence, metabolic interactions between OPTs are known and here interaction between Pho and CPF were tested. When Pho (0–60 μM) was used as a mechanism-based inhibitor, the formation of CPF metabolites CPFO and TCP with HLM was monitored at 6 different substrate concentrations (15–300 μM). The Michaelis–Menten plot for TCP formation evidenced that Vmax was reduced by increasing inhibitor (Pho) concentration, whilst Km was not affected (Fig. 6A). This behavior is typical of mechanism–based as well as non-competitive inhibition. In fact, the best

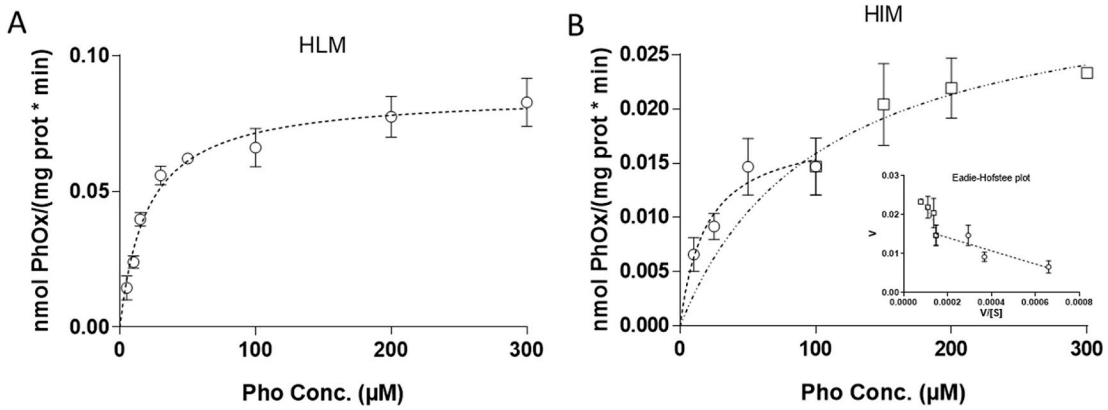

Fig. 4. Dependence of Pho metabolism catalysed by HLM (A) and HIM (B) on substrate concentration. The inset of panel B shows the Eadie–Hosftee plot (V vs. V/S) for HIM data. Results are expressed as nmol PhOx (mg protein · min)$^{-1}$ and represent the mean ± SD on at least 3 independent experiments with the same pool. Details of the experimental conditions were described under Materials and Methods.

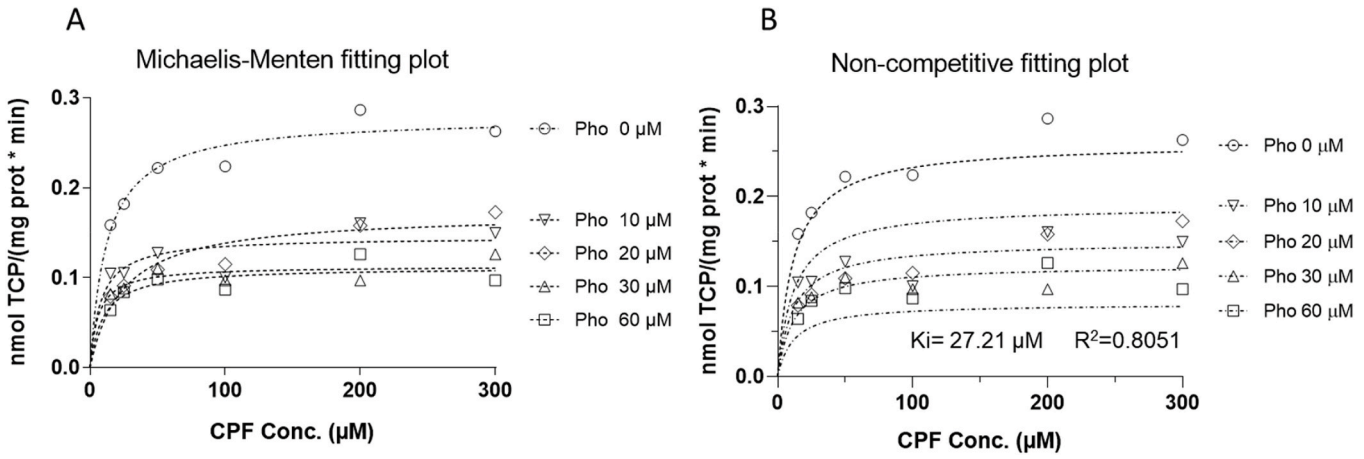

Fig. 6. Metabolic interaction between Pho and CPF in HLM: inhibition of TCP formation by different Pho concentrations in HLM. The Michaelis-Menten plot (A) and the best fitting (B) obtained for the non-competitive mechanism are shown. Results represent the mean value on at least 3 independent determinations on a pool from 200-donors. Details of the experimental conditions were described under Materials and Methods.

fit of the plot was obtained using a non-competitive inhibition (R^2 = 0.8051) allowing to derive a Ki = 27.2 μM (Fig. 6B).

No CPFO formation was detectable below 100 μM CPF, even at the lowest inhibitor concentrations. At higher CPF concentration, the Michaelis-Menten plot for CPFO formation evidenced an increase in Km values dependent on the inhibitor concentration, whilst Vmax values were almost unchanged (Fig. 7A). This indicate that Pho acts as a competitive inhibitor, as conformed by the best fit (R^2 = 0.9253) from which a Ki = 29.66 μM was extrapolated (Fig. 7 B).

The IC_{50} value was calculated from the linear regression obtained by plotting the inhibition (%) vs inhibitor concentration (Fig. 8A): parallel straight lines for CPFO formation were obtained, indicating that the IC_{50} values depend on CPF concentrations (IC_{50} = 59, 87 and 115 μM, at 100, 200 and 300 μM CPF, respectively). With TCP the IC_{50} values were independent of substrate concentrations (Fig. 8B) and IC_{50} = 28 ± 8 μM (mean ± SD) was calculated. The value is almost identical to Ki, as it is generally demonstrated for non-competitive inhibitors.

CPF (25–300 μM) was tested both as a mechanism-based inhibitor (using pre-incubation) and as a competitive inhibitor (adding it together with 30 and 100 μM Pho). Results showed that the inhibition of PhOx was independent on the type of incubation. Indeed, Pho bioactivation was only partially reduced (≤50%), even at the highest CPF concentration tested (300 μM) and associated with IC_{50} = 340 ± 46 μM, and Ki = 159.6 μM, calculated by means of the Dixon Plot.

4. Discussion

There is an increasing demand in quantitative risk assessment for a shift towards the use of mechanistic data obtained with animal-free methods, while considering inter-individual differences in kinetic processes and metabolism. Kinetics and metabolism data are fundamental to researchers and risk assessors to further refine the calibration of physiologically-based kinetic models with more robust data. Information on isoform-specific biotransformation in human samples with related parameters (e.g. Vmax, Km and Cli) are fundamental for such refinement. Here, isoform-specific desulfuration of Pho to the corresponding toxic metabolite, PhOx, has been characterized *in vitro* for the first time, using a broad range of Pho concentrations (0.5–300 μM).

When conducting these studies, the use of *in vitro* concentrations related to the actual human exposure is crucial to generate data relevant to the in vivo situation. It has been previously suggested that *in vitro* concentrations of OPTs≤ 10 μM are the most appropriate to simulate in vivo exposures (Buratti et al., 2003, 2005). In fact, plasma concentration data, biomonitoring data or pharmacokinetic models obtained for other OPTs such as chlorpyrifos, azynphos methyl or malathion support the suggestion (Carrier and Brunet, 1999; Kutz et al., 1992; Rigas et al., 2001; Schurdut et al., 1998). Since in vivo hepatic

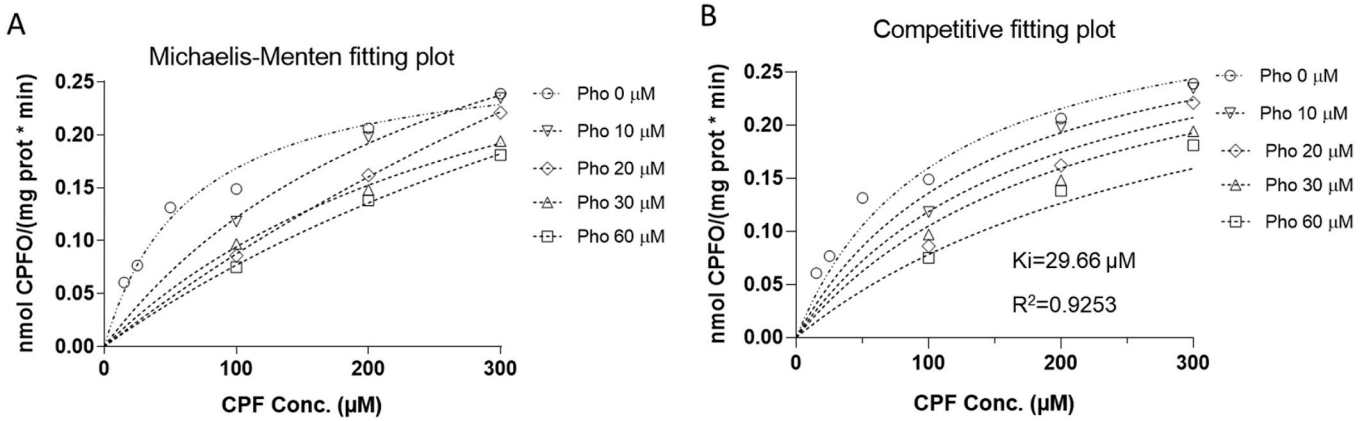

Fig. 7. Metabolic interaction between Pho and CPF in HLM: inhibition of CPFO formation by different Pho concentration in HLM. The Michaelis-Menten plot (A) and the best fitting obtained for the competitive mechanism (B) are shown. Results represent the mean value on at least 3 independent determinations on a pool from 200-donors. Details of the experimental conditions were described under Materials and Methods.

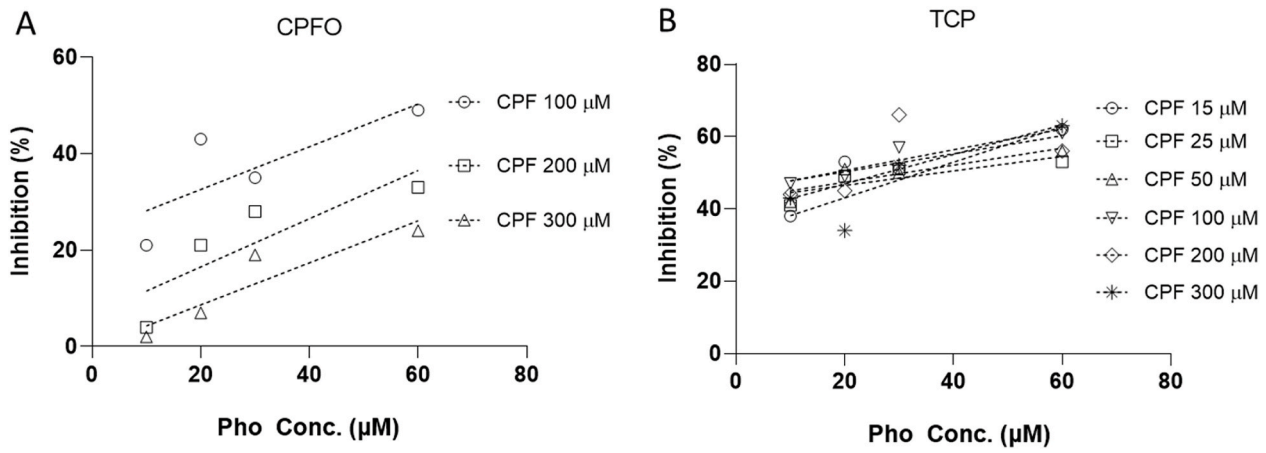

Fig. 8. IC50 for Pho inhibition of CPFO (A) and TCP (B) formation in HLM. Results represent the mean value on at least 3 independent determinations on a pool from 200-donors.

concentrations are usually higher than circulating ones, Pho concentrations ≤50 μM can be easily achieved in exposed individuals, and therefore, the *in vitro* concentrations that have been used in these experiments can be considered as relevant and representative of human exposure scenarios.

All CYPs tested, except CYP2C8 were active: CYP2C18 and 2C19 showed the highest affinity for Pho (meaning the lowest Km values), the highest Vmax and consequently the highest Cli values, with other CYPs, particularly CYP2B6, also showing a significant bioactivation activity. Despite this, a more realistic picture of their relative role should take into account also CYP hepatic content: the extrapolation evidenced that CYP2C18, the one characterized by the highest Cli, gave only a minor contribution, and in addition CYPs have a different role depending on Pho concentrations. This feature has been previously evidenced with other OPTs studied in our laboratory (Buratti et al., 2002, 2003; 2005; Leoni et al., 2008). However, differently from all the previously studied OPTs, for which CYP2B6 and CYP1A2 were the isoforms mainly involved in oxon formation at low insecticide concentrations, the CYP2C family accounted for the great majority (76%) of the oxidative desulfuration of Pho with i) a prominent role for CYP2C19 (60%), ii) CYP2B6 being responsible for the remaining activity (20%) and iii) CYP1A2 giving a very limited contribution. At higher OPTs concentrations, the trend described for the other OPTs was confirmed also for Pho, i.e. a more widespread CYP involvement, with CYP3A4 and the CYP2C family playing the major role.

The lower catalytic efficiency of HLM compared to the recombinant enzymes can be attributed to the competition among the different isoforms which are concurrently present and compete with each other for the substrate. In addition, although a single straight line was evidenced with the Eeadie–Hofstee plot (data not shown), indicating a similar contribution of all isoforms in the range of tested concentration, the use of specific chemical inhibitors allowed to confirm the different role of specific CYPs at different Pho concentrations as described above. In order to further substantiate these results, the Relative Abundance (RA) approach (Stringer et al., 2009) was also used and again a predominant role for CYP2C19 was predicted with the highest CLi_{CYP} (Table 3).

With HIM, the obtained atypical kinetic curve was initially interpreted as due to auto-activation, looking at results obtained with the recombinant CYP3A4 and in analogy of what we have previously reported for dimethoate desulfuration (Buratti and Testai, 2007). However, the allosteric curve fitting was poor and a Hill coefficient < 1 (0.55) was obtained, indicative of negative cooperativity (data not shown). The situation was clarified by the double straight lines obtained in the Eadie–Hostee plot (instead of the 'hockey stick' curve typical of auto-activation), clearly indicating that the reaction was characterized by two different phases, associated to enzymes with

Table 3
Relative abundance and CLiCYP in HLM.

CYPs	RA[a]	Cl_{iCYP}[b]
2C18	0.34	0.3
2C19	9	4.4
2B6	14	1.5
2C9	53	0.9
1A1	1	0.01
1A2	34	0.1
2D6	11	0.02
3A4	80	0.1
2A6	23	0.01
2C8	19.3	–

Total HLM P450 concentration = 335 pmolP450/mg prot.
Relative Abundance (RA) for a CYP is the ratio: (Total HLM CYP450 concentration/100) * A, where A is the % content of the CYP in HLMs (extrapolated from Achour et al., 2014 and Pastrakuljic et al., 1997).
CliCYP related to PhOx formation in HLM for each isoform was calculated as: PhOx-ClirecCYP * RA (Stringer et al., 2009).
[a] = pmolCYP/mg prot.
[b] = pmol product/(mg prot · min · μM) (microsomal CLint contributions for PhOx from each CYPs).

different affinity for Pho. The atypical kinetic curve was indeed due to the overlapping of two Michaelis-Menten curves (Fig. 4B), corresponding to CYPs mainly present in the gut: CYP3A4 and 2C family (2C9 and 2C19) accounting for > 80% and about 18% of the total CYP content, respectively (Paine et al., 2006). The high affinity phase was mainly catalysed by the CYP2C family, while at increasing Pho concentration (≥100 μM), when CYP2C isoforms are saturated, the major contribution was given by CYP3A4. The catalytic efficiency associated with the high affinity phase was around 23% of the hepatic one, therefore the role of the gut pre-systemic bioactivation cannot be dismissed, especially at low exposure levels.

Exposure data in cohorts of population which live mainly in rural communities (Butler-Dawson et al., 2018) evidenced the actual co-exposure to Pho and other pesticides (mainly OPTs) which are detected in house dust and as urinary metabolites (Coronado et al., 2011; Fenske et al., 2000; Gunier et al., 2011). It is therefore important to investigate the possible metabolic interactions between multiple OPTs at relevant levels of human exposure. The only partial inhibition of PhOx formation (max 50%) also at relatively high CPF concentrations (with high IC_{50} e Ki values) can be explained with the involvement of CYP2C19 in Pho bioactivation. Indeed, the mechanism-based CYP inhibition is mediated by CPFO formation, which is catalysed by CYPs other than CYP2C19 (Buratti et al., 2002), which is therefore only partially affected. In CPF metabolic pathway, CYP2C19 is known to catalyse TCP

formation, without enzyme inactivation (Buratti et al., 2002; Tang et al., 2001). This consideration is consistent with results obtained by using Pho as an inhibitor. PhOx formation also at relatively low concentrations, causing CYP2C family and CYP2B6 inactivation, efficiently inhibited TCP as well as CPFO formation, respectively, with Ki values around 30 μM, concentration which are likely to be attained in the liver of exposed individuals. On the contrary, the Ki value associated to CPF inhibition of Pho bioactivation was relatively high (≈160 μM), much higher than the concentration achievable in vivo, and therefore they were considered of limited relevance.

Consequently, despite the generic common metabolic pathway for OPTs, involving the oxidative desulfuration mediated by CYPs, isoform-specific metabolic interactions may occur, depending on i) the variability in the CYP activity and efficiency to form the oxon, ii) the inactivation of the enzyme itself, which in turns may modulate the toxicity of chemicals in combined exposure scenarios.

For this reason, kinetics and mode of action information for active substances is fundamental to improve human risk assessment of pesticides, other regulated compounds (food and feed additives, flavourings) as well as food contaminants (e.g mycotoxins, persistent organic pollutants etc) (EFSA, 2018). In addition, such information provides a basis to investigate metabolic interactions between multiple chemicals that may involve either inhibition or induction of metabolism and allow to identify possible sensitive subgroups within the population. Our data also evidenced the importance of considering the pre-systemic bioactivation in the gut, especially when the involved enzymes are polymorphic, as in the case of Pho and CYP2C19. Such isoform-specific kinetic information can be combined with variability distributions, describing inter-individual differences in CYP activities and support the development of quantitative *in vitro/in vivo* extrapolation (QIVIVE) models and PBK models for the refinement of the human risk assessment for single chemicals. With regards to multiple chemicals, such QIVIVE and PBK models can be further calibrated with metabolic interaction data, to investigate the consequence of inhibition or induction of isoform-specific metabolism on either bioactivation or detoxification as well as the potential implications on the toxicodynamics of the compounds.

5. Conclusions

The characterization of the *in vitro* isoform-specific bioactivation of Phosmet in liver and intestinal samples of human origin, evidenced that CYP2C19 contributed for the great majority to the formation of the neurotoxic metabolite oxon at relevant exposure concentrations. This feature was not shared by other OPTs, for which CYP1A2 and CYP2B6 were the most active CYPs in forming the corresponding oxon at low exposure concentration. We also evidenced the relevance of pre-systemic Pho bioactivation in the gut, accounting for ¼ of that measured in the liver, due to the presence of CYP2C and CYP3A4 in the gut. Phosmet can efficiently inhibit both CPF bioactivation and detoxication, while the opposite is not relevant at the actual exposure levels, again depending on the peculiar isoform-specific Pho bioactivation when compared to other OPTs. Our data highlight the relevance of generating kinetic information for improving human risk assessment of single pesticides (and their mixtures) as well as other compounds, describing potential inter-individual differences and supporting the development of QIVIVE and PBK models to face a risk assessment in an animal free environment.

Disclaimer

The views in this publication do not necessarily represent those of EFSA and are the authors only.

CRediT authorship contribution statement

Nicoletta Santori: Investigation, Formal analysis, Writing - original draft. **Franca Maria Buratti:** Conceptualization, Formal analysis, Visualization, Writing - original draft, Writing - review & editing. **Jean-Lou C.M. Dorne:** Writing - review & editing, Project administration. **Emanuela Testai:** Conceptualization, Supervision, Writing - review & editing, Project administration.

Declaration of competing interest

The authors declare that they have no known competing financial interests or personal relationships that could have appeared to influence the work reported in this paper.

Acknowledgments

This project was partially supported by:

- the European Food Safety Authority (EFSA) under the grant agreement no. GA/EFSA/SCER/2015/01.

- Collaboration Agreement between Italian Ministry of Health and Istituto Superiore di Sanità , Grant n°4S05.

References

Achour, B., Barber, J., Rostami-Hodjegan, A., 2014. Expression of hepatic drug-metabolizing cytochrome P450 enzymes and their intercorrelations: a meta-analysis. Drug Metab. Dispos. 42, 1349–1356.

Aprea, C., Sciarra, G., Sartorelli, P., 1998. Environmental and biological monitoring of exposure to mancozeb, ethylenethiourea, and dimethoate during industrial formulation. J. Toxicol. Environ. Health 53, 263–281.

Aprea, C., Terenzoni, B., De Angelis, V., Sciarra, G., Lunghini, L., Borzacchi, G., Vasconi, D., Fani, D., Quercia, A., Salvan, A., Settimi, L., 2004. Evaluation of skin and respiratory doses and urinary excretion of alkylphosphates inworkers exposed to dimethoate during treatment of olive trees. Arch. Environ. Contam. Toxicol. 48, 127–134.

Buratti, F.M., Volpe, M.T., Fabrizi, L., Meneguz, A., Vittozzi, L., Testai, E., 2002. Kinetic parameters of OPT pesticide desulfuration by c-DNA expressed human CYPs. Environ. Toxicol. Pharmacol. 11, 181–190.

Buratti, F.M., Volpe, M.T., Meneguz, A., Vittozzi, L., Testai, E., 2003. CYP-specific bioactivation of four organophosphorothionate pesticides by human liver microsomes. Toxicol. Appl. Pharmacol. 186, 143–154.

Buratti, F.M., D'Aniello, A., Volpe, M.T., Meneguz, A., Testai, E., 2005. Malathion bioactivation in the human liver: the contribution of different cytochrome P450 isoforms. Drug Metab. Dispos. 33, 295–302.

Buratti, F.M., Leoni, C., Testai, E., 2006. Foetal and adult human CYP3A isoforms in the bioactivation of organophosphorothionate insecticides. Toxicol. Lett. 167 (3), 245–255.

Buratti, F.M., Testai, E., 2007. Evidences for CYP3A4 autoactivation in the desulfuration of dimethoate by the human liver. Toxicology 241 (1–2), 33–46.

Butler, A.M., Murray, M., 1997. Biotransformation of parathion in human liver: participation of CYP3A4 and its inactivation during microsomal parathion oxidation. J. Pharmacol. Exp. Therapeut. 280, 966–973.

Butler-Dawson, J., Galvin, K., Thorne, P.S., Rohlman, D.S., 2018. Organophosphorus pesticide residue levels in homes located near orchards. J. Occup. Environ. Hyg. 15 (12), 847–856.

Carrier, G., Brunet, R.C., 1999. A toxicokinetic model to assess the risk of azinphosmethylexposure in humans through measures of urinary elimination of alkylphosphates. Toxicol Sci 47, 23–32.

Coronado, G.D., Holte, S., Vigoren, E., Griffith, W.C., Barr, D.B., Faustman, E., Thompson, B., 2011. Organophosphate pesticide exposure and residential proximity to nearby fields: evidence for the drift pathway. J. Occup. Environ. Med. 53 (8), 884–891.

EFSA Journal, 2011. Conclusion on the Peer Review of the Pesticide Risk Assessment of the Active Substance Phosmet, vol. 9. pp. 2162 5.

EFSA (European Food Safety Authority) Journal, 2018. Draft guidance on harmonised methodologies for human health, animal health and ecological risk assessment of combined exposure to multiple chemicals. Available at: https://www.efsa.europa.eu/sites/default/files/consultation/consultation/180626-1-ax1.pdf.

Fenske, R.A., Kissel, J.C., Lu, C., Kalman, D.A., Simcox, N.J., Allen, E.H., Keifer, M.C., 2000. Biologically based pesticide dose estimates for children in an agricultural community. Environ. Health Perspect. 108 (6), 515–520.

Gunier, R.B., Ward, M.H., Airola, M., Bell, E.M., Colt, J., Nishioka, M., Buffler, P.A., Reynolds, P., Rull, R.P., Hertz, A., Metayer, C., Nuckols, J.R., 2011. Determinants of agricultural pesticide concentrations in carpet dust. Environ. Health Perspect. 119 (7), 970–976.

Halpert, J.A., Hammond, D., Neal, R.A., 1980. Inactivation of purified rat liver cytochrome P-450 during the metabolism of parathion (diethyl-p-nitrophenyl-phosphorothionate). J. Biol. Chem. 255, 1080–1089.

Kappers, W.A., Edwards, R.J., Murray, S., Boobis, A.R., 2001. Diazinon is activated by CYP2C19 in human liver. Toxicol. Appl. Pharmacol. 177, 68–76.
Kutz, F., Cook, B.T., Carter-Pokras, O.D., Brody, D., Murphy, R.S., 1992. Selected pesticide residues and metabolites in urine from a survey of the US general population. J Toxicol Environ Health 37, 277–291.
Leoni, C., Buratti, F.M., Testai, E., 2008. The participation of human hepatic P450 isoforms, flavin-containing monooxygenases and aldehyde oxidase in the biotransformation of the insecticide fenthion. Toxicol. Appl. Pharmacol. 233 (2), 343–352.
Mutch, E., Blain, P.G., Williams, F.M., 1999. The role of metabolism in determining susceptibility to parathion toxicity in man. Toxicol. Lett. 107, 177–187.
Norman, B.J., Poore, R.F., Neal, R.A., 1974. Studies of the binding of sulfur released in the mixed-function oxidase-catalysed metabolism of diethyl p-nitrophenyl phosphorothioate (parathion) to diethyl p-nitrophenyl phosphate (paraoxon). Biochem. Pharmacol. 23, 1733–1744.
Paine, M.F., Hart, H.L., Ludington, S.S., Haining, R.L., Rettie, A.E., Zeldin, D.C., 2006. The human intestinal cytochrome P450 "pie. Drug Metab. Dispos. 34 (5), 880–886.
Pastrakuljic, A., Tang, B.K., Roberts, E.A., Kalow, W., 1997. Distinction of CYP1A1 and CYP1A2 activity by selective inhibition using fluvoxamine and isosafrole. Biochem. Pharmacol. 53 (4), 531–538.
Rigas, M.L., Okino, M.S., Quackenboss, J.J., 2001. Use of pharmacokinetic model to assess chlorpyrifos exposure and dose in children, based on urinary biomarker measurement. Toxicol. Sci. 61, 374–381.
Sánchez-Santed, F., Colomina, M.T., Herrero Hernández, E., 2016. Organophosphate pesticide exposure and neurodegeneration. Cortex 74, 417–426.
Schurdut, B.A., Barraj, L., Francis, M., 1998. Aggregate exposures under the food quality protection act: an approach using chlorpyrifos. Regul. Toxicol. Pharmacol. 28, 165–177.
Stringer, R.A., Strain-Damerell, C., Nicklin, P., Houston, J.B., 2009. Evaluation of recombinant cytochrome P450 enzymes as an in vitro system for metabolic clearance predictions. Drug Metab. Dispos. 37, 1025–1034.
Tang, J., Cao, Y., Rose, R.L., Brimfield, A.A., Dai, D., Goldstein, J.A., Hodgson, E., 2001. Metabolism of chlorpyrifos by human cytochrome P450 isoforms and human, mouse and rat liver microsomes. Drug Metab. Dispos. 29, 1201–1204.